Polymer Degradation and Stability 124 (2016) 35–42

Contents lists available at ScienceDirect

Polymer Degradation and Stability

journal homepage: www.elsevier.com/locate/polydegstab

Water immersion aging of polydicyclopentadiene resin and glass fiber composites

Yinghui Hu*, Xiaochen Li, Augustus W. Lang, Yunpeng Zhang, Steven R. Nutt

M.C. Gill Composites Center, Department of Chemical Engineering and Materials Science, University of Southern California, Los Angeles, CA 90089, USA

ARTICLE INFO

Article history:
Received 12 July 2015
Received in revised form
10 October 2015
Accepted 8 December 2015
Available online 12 December 2015

Keywords:
Polymer-matrix composites (PMCs)
Environmental degradation
Fiber–matrix interface

ABSTRACT

We present an investigation of the effect of long-term water immersion aging on the thermal/mechanical properties of a ruthenium-catalyzed polydicyclopentadiene (pDCPD) polymer and associated composites, using an epoxy resin system as a benchmark. The pDCPD neat polymer showed low-level water absorption after one year of aging due to inherent hydrophobicity. No plasticization was observed for pDCPD, while significant plasticization occurred for the epoxy. Salt water aging and deionized water aging had identical effects on pDCPD and composites, while epoxy materials aged in salt water showed less water absorption compared to aging in deionized water. We also measured the fiber-interface strength before and after aging of composites using single-fiber push-out tests. Aging caused decreases in interface strength, and these decreases led to a decline in composite fatigue strength.

1. Introduction

Polymer composites are widely employed in aerospace structures [1], and composite applications have begun to expand in non-aerospace sectors as manufacturing technology advances and manufacturing costs decline [2,3]. In both aerospace and non-aerospace sectors, which include marine, civil infrastructure and energy applications, long-term durability is a major concern. In such applications, materials are often required to function in service conditions that involve exposure to multiple, often simultaneous, factors that cause aging in polymeric composites, including high/low temperatures, moisture, ultra-violet, oxidation, freeze-thaw cycling, and cyclic loads. Furthermore, components are expected to provide decades of uninterrupted service with minimal inspection or maintenance. For example, wind turbine blades must function in aggressive service environments in which multiple aging factors operate, including fatigue loading, sunshine, temperature cycling, and oxidation. For off-shore wind farms, moisture and salt corrosion pose additional durability challenges for polymer composites.

Multiple studies have reported the accelerated aging behavior of polymers and composites, providing useful insights. However, the material response is often complex, and fundamental behavior that stems from coupled aging factors remains largely beyond our understanding. For example, in marine applications [4–6], aging mechanisms include differential swelling, residual stress relaxation, and hydrolysis. Cracking, creep, leaching, post-crystallization and even biodegradation may occur simultaneously or successively. The current study focuses on one major aging factor - moisture - and investigates its effect on mechanical performance. Common practice in aging research is to increase exposure temperatures to accelerate moisture aging because low temperature (room temperature) aging generally requires prohibitively long times to cause observable changes in properties [7].

Hygrothermal aging causes important changes to polymer composites, often limiting service life and restricting applications [8–26]. For example, the polymer matrix can undergo plasticization when a moderate amount of water is absorbed [8,9], increasing chain mobility and decreasing glass transition temperature, stiffness, and strength, while also increasing fracture toughness [10]. Physical aging occurs simultaneously, regardless of moisture level [27–29]. Physical aging is a structural relaxation process and a movement toward equilibrium state, in which the free volume shrinks. Physical aging increases stiffness, strength, and chemical resistance, while decreasing ductility. Aging often results in degradation of the fiber–matrix interface and is thus a major factor that reduces the overall mechanical performance of composites [11,12]. In fact, interface damage reportedly is often the dominant mode of damage in both static and fatigue failure of aged composites [13–15].

* Corresponding author.
E-mail address: yinghuih@usc.edu (Y. Hu).

http://dx.doi.org/10.1016/j.polymdegradstab.2015.12.008
0141-3910/

Polydicyclopentadiene (pDCPD) reportedly shows superior thermal stability and chemical corrosion resistance relative to most other polymers [16–18], and thus is a potential candidate for emerging composite applications outside of aerospace, such as wind turbine blades. Other advantages include intrinsic hydrophobicity controllable curing rate, and low liquid viscosity which facilitates infiltration during manufacture. However, the long-term durability of pDCPD under aging conditions of moisture, high temperature and oxidation has not been thoroughly investigated. Le Gac et al. [16] studied the aging effect of natural seawater on neat pDCPD resin at 90°C-180 °C for up to 18 months, and reported that aging effects were localized to a thin surface layer in aging environments below T_g where aging was diffusion-limited. They also reported no evidence of hydrolysis in any environmental condition, indicating the exceptional moisture-resistance of this material. However, seawater aging above T_g caused effects throughout the bulk of the composite. The superior thermal stability [17] and abrasive friction resistance [18] of pDCPD also was confirmed in other reports. In recent years, a new formulation of pDCPD (Proxima™, Materia, Inc.) using ruthenium as catalyst was developed. This formulation has shown promising toughness, high chemical resistance, and low viscosity, although the long-term hygrothermal aging behavior has not yet been reported.

In this study, we investigated the effect of water immersion aging on this new pDCPD polymer (Proxima, Materia, Inc.) and associated composites, using a traditional epoxy resin as a benchmark. After aging in deionized water and salt water, we used thermal mechanical analysis (DMA) to characterize the thermomechanical properties, and various mechanical test methods were used to evaluate the evolution of mechanical performance. In the Results and Discussion section, the effects of aging on the composite matrix, fiber and interface are presented, and the degradation effects on the overall composite fatigue behavior are assessed. (Detailed analysis of the fatigue behavior appears elsewhere [19]). The results reveal that low moisture absorption is critical to the retention of thermal and mechanical properties for pDCPD materials after aging. Analysis of the results demonstrates that these factors must be taken into account when designing components for composite applications involving hygrothermal service conditions.

2. Experimental

2.1. Sample preparation

The pDCPD neat polymer (Proxima™, Materia, Inc., Pasadena, CA) and unidirectional (UD) glass fiber composite samples were manufactured using conventional vacuum infusion techniques. E-glass fiber was selected (94 wt% PPG Hybon® 2026 in the warp direction and 6 wt% PPG Hybon® 2002 in the weft direction). The density of glass fibers was 2.63 g/cm^3 (from the manufacturer) and fiber volume fractions were ~58%, determined from burn-out tests. Both neat polymer and composite samples were cured at 30 °C for 2 h, then at 100 °C for 30 min, per manufacturer's specification.

An epoxy resin system widely used for wind turbine blades was selected as a benchmark material (Epikote™ 135 resin with 137 hardener, Momentive, Inc.), and samples were prepared in the same way as pDCPD samples, although the epoxy samples were cured at 80 °C for 8 h Table 1 shows the basic properties of the two cured resins. Measurement of T_g were performed by DMA, as described below, and mechanical properties were measured by quasi-static tensile tests, also described below.

2.2. Aging conditions

Two aging environments were used to compare the effects of pure water and salt water aging: (1) immersion in deionized water at 60 °C, and (2) immersion in 3.5 wt% NaCl water solution at 60 °C. The chosen temperature was sufficient to cause observable changes in properties, yet insufficient to activate aging mechanisms operative only near or over T_g (Table 1) [16]. Condition (1) is hereafter referred as "DI water", and condition (2) is referred to as "salt water". The samples were immersed in water storage tanks (500 × 250 × 200 mm, *length* × *width* × *height*) and the aging solution was refreshed every week. The solution was exposed to air, allowing for dissolution of oxygen, although no bubbling was used to expedite the oxidation process.

2.3. Dynamic mechanical analysis (DMA)

Dynamic mechanical analysis (DMA, TA Instruments, Q800) was conducted to monitor the change in glass transition temperature (T_g) and thermomechanical properties after aging. A single cantilever beam sample was used (ASTM D7028), and samples were cut from 4-ply composite laminates to standard dimensions (35 × 12 × 3.2 mm, *length* × *width* × *thickness*). The temperature was ramped from 40 °C to 160 °C at a rate of 5 °C/min. A loading frequency of 1 Hz and strain amplitude of 2 μm were used, and the storage modulus, loss modulus and tan(δ) curves were recorded.

2.4. Fracture toughness

The fracture toughness of neat polymer samples was measured to determine the effects of hygrothermal aging (plasticization or strengthening). Tests were conducted in accordance with ASTM D5045, and test samples were single-edge-notch beams (SENB). The dimensions of the SENB samples were 80 × 16 × 8 mm (*length* × *width* × *thickness*), determined by several iterations of trial tests to yield valid measurements. Neat polymer dogbone samples (ASTM D638) were also aged and tested in tension for validation purposes. The dimensions of the dogbone sample were 70 × 10 × 4 mm (*gauge length* × *width* × *thickness*).

The SENB samples were first notched and pre-cracked, then loaded in 3-point bending (3 PB) to failure using a load frame (Instron 5567). The notch and pre-crack were created after aging to avoid blunting during aging. The span length of the 3 PB fixture was 32 mm, and the loading rate was 10 mm/min. At least three samples with valid results were tested per test condition to yield reliable data. The load–displacement curve was recorded to calculate mode I fracture toughness (K_{IC}).

2.5. Quasi-static tension

Tensile tests of 0° composite samples were conducted according to ASTM D3039 using a load frame (Instron 5585H). Samples were

Table 1
Basic properties of cured pDCPD and epoxy neat polymer.

	T_g (°C)	Density (g/cm^3)	Tensile modulus (GPa)	Ultimate tensile strength (MPa)	Tensile elongation
pDCPD	124	1.05	3.1	73	2.7%
epoxy	101	1.15	2.9	64	3.4%

cut from 2-ply composite laminates to dimensions 200 × 25 × 1.6 mm (*length* × *width* × *thickness*). Tabs on both ends and on both sides of the sample were used to prevent stress concentration and failure in the grips during testing. The dimensions of the tab were 50 × 25 × 3.2 mm (*length* × *width* × *thickness*). Samples were loaded in tension at a rate of 2 mm/min until rupture, and at least five samples were tested per test condition. An extensometer (Instron 2630-109) was clipped onto the gauge length of the sample to measure extension. Load and strain were recorded, while elastic modulus, ultimate tensile strength and elongation were determined/calculated after testing.

2.6. Short-beam shear

The interlaminar shear strength (ILSS) was evaluated by conducting short-beam shear (SBS) tests according to ASTM D2344. Samples were cut from 4-ply laminates to dimensions of 19 × 6.4 × 3.2 mm (*length* × *width* × *thickness*), and the fiber direction was along the length direction. Samples were loaded in 3-point bending (3 PB) at a loading rate of 1 mm/min until first failure occurred, and at least five samples were tested per test condition. The span of the 3 PB fixture was set to 12.7 mm, in accordance with the test standard.

2.7. Fiber push-out

Unlike most methods for quantitative measurement of interface strength [30–34] (including fiber pull-out, fiber fragmentation, micro-droplet tensile test), the fiber push-out method [32–34] does not require preparation of single-fiber composites. The push-out test also affords the ability to make measurements on fibers in samples with process histories (and aging histories) identical to those of bulk composites. In the test, a thin section (~ 10 × the fiber diameter) is prepared transverse to the fiber direction, and a single fiber is pushed out using a truncated cone indenter. Fig. 1 shows an image after interface slippage during a push-out test on a glass fiber-pDCPD composite. The load, time and displacement are recorded during the test, and the apparent interface shear strength τ_{app} is calculated using Eqn. (1):

$$\tau_{app} = \frac{F}{\pi DL} \quad (1)$$

in which F is the load when push-out occurs, D is the fiber diameter, L is the fiber length (i.e., sample thickness).

The push-out test apparatus resides in a scanning electron microscope (SEM, JEOL JSM-6610LV) and consists of a diamond tip (Hysitron, 10 μm tip diameter), a load sensor (Honeywell FSG020, resolution 0.4 mN, range ±5 N), a driving motor (McLellan, resolution 0.25 μm), a sample support, an I/O interface (National Instruments), and control software (LabView). The tester is built on.

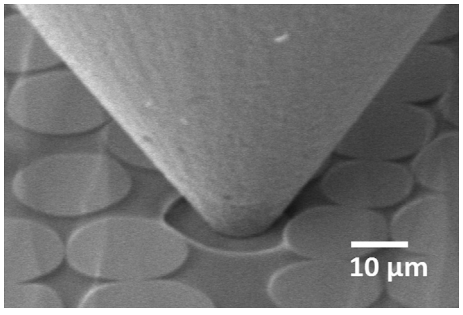

Fig. 1. Fiber push-out of glass/pDCPD composite.

The sample is supported on an aluminum stub with 0.5 mm grooves. Fibers in the groove region can be pushed out without resistance from the aluminum support platform. To prepare the sample, a thin section (~1 mm) is cut transverse to the fiber direction, and both sides are abrasively polished. The target sample thickness for glass fiber composites is 100 μm. The fiber diameter is measured directly from the SEM image.

2.8. Fatigue

Tension–tension fatigue tests were conducted on 0° composites using a hydraulic load frame (Instron 8500R-1331) in air in a well-ventilated room to study the effects of aging. Samples were identical to those used for 0° quasi-static tensile tests, and tests were conducted following ASTM D3479 (for testing) and ASTM E739 (for data interpretation). Experiments were conducted under load control, and the stress ratio R was set to 0.1, which is a commonly used value for tensile fatigue of polymer composites [3,19]. A loading frequency of 5 Hz was used, which is not low enough to avoid significant heating of the sample. The maximum temperature rise was less than 3 °C, monitored by a thermocouple attached to the sample surface. Samples were cycled to rupture, and the cycles to failure (N) was recorded together with the stress (S) applied. If the sample did not fail after 10^6 cycles, the test was terminated because of time limit. This cycle number is described as run-out cycle. By summarizing the S–N curves from different aging times, environments and matrix, we can analyze the effect of aging type and time on the fatigue behavior of the different composites.

3. Results and discussion

3.1. Matrix degradation

Fig. 2 shows the weight change for different samples in the two aging environments for aging periods up to one year. Samples were first wiped dry before weighing on a digital scale. Five samples per condition were measured and the standard deviation was less than 10%. The sampling points are 0, 1, 3, 6 and 12 months and they share the same symbol definitions as in Fig. 2b.

Fig. 2a shows that SENB samples of pDCPD neat resin exhibited a slight decrease in weight in the first month, then gradually gained weight over the following 11 months. Saturation was not reached despite aging for one year. Note that water absorption is not equal to weight change because other mechanisms affecting sample weight, such as oxidation and leaching, can operate concurrently. The weight decrease noted in the first month was attributed to small molecules, such as DCPD monomers and oligomers, diffusing out of the sample. The subsequent weight increase was caused by molecular water diffusion into the polymer network (water molecules can exist in a free or bound state with the polymer chains). In comparison, epoxy samples showed much faster and greater weight gain and approached saturation after twelve months of aging. While small molecules may diffuse out of the sample, this effect was more than compensated by the much faster and concurrent water absorption process. The significant difference in the amount of water absorbed by pDCPD and epoxy resins is readily explained by the intrinsic hydrophobicity of pDCPD and the hydrophilic hydroxyl groups in epoxy networks. The addition of salt to the aging solution led to reduced water absorption for the epoxy samples, which was attributed to a lower water activity in the presence of salt. In contrast, pDCPD samples showed negligible weight change during salt water aging.

Fig. 2b shows the weight change of 4-ply composite laminates. Note that 4-ply laminates (200 × 200 × 3.2 mm, *length* × *width* × *thickness*) were first aged, then sliced into tensile

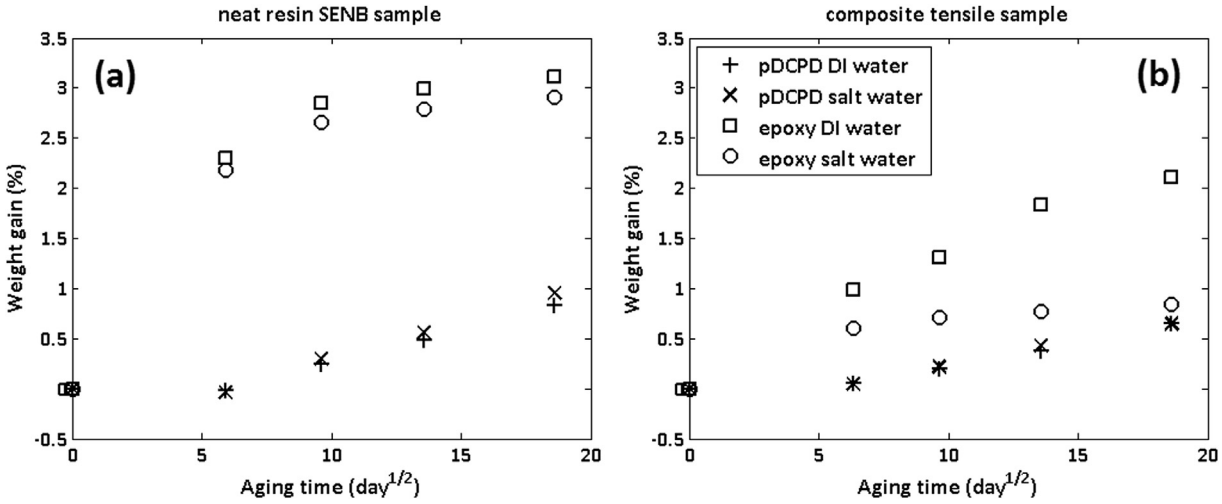

Fig. 2. Weight change during aging.

coupons just prior to testing. Thus, the water diffusion mechanism for these laminates was identical to that for the neat polymer. The one exception was that the epoxy composite showed much greater water absorption when aged in DI water compared to aging in salt water, and the difference was greater for the epoxy composites than for the neat polymer samples. This phenomenon can only be explained by an additional mechanism for water diffusion and storage operating in the composites - capillary diffusion along debonded fiber–matrix interfaces [11]. (The possibility of water absorption by voids was discounted because voids were not detected in microscopic examinations of polished sections of both composites.)

By comparing Fig. 2a and b, we can evaluate the influence of the fiber–matrix interface on water absorption in the composites, assuming that glass fiber does not absorb water. After one year of aging in DI water, the weight gain of pDCPD neat resin is 0.83% while the weight gain of pDCPD composite is 0.65%. If we assume the composite matrix gained the same percentage as in the neat resin and use the measured fiber volume fraction, the weight gain contribution from the matrix should be 0.2%. Thus, the weight gain from sources other than matrix swelling for the pDCPD composite is 0.45%. Using the same calculation procedure, the weight gain from sources other than matrix swelling for the epoxy composite is 1.36%. These sources primarily include water uptake by interfaces and oxidation on sample surfaces. If we assume that the weight gain from oxidation is similar for both composites (based on similar geometry), the greater water uptake by epoxy composites can be attributed to absorption at interfaces.

Fig. 3 shows the tan(δ) curves for the two composites as a function of temperature for different aging times. The T_g of the pDCPD samples increased slightly after two months of aging, then remained constant during additional aging. At the same time, the peak height and width of the tan(δ) curve decreased monotonically with increasing aging, indicating diminishing chain mobility. The slight increase in T_g within the first two months can be attributed to post-curing, thermal effects and/or surface oxidation. After this initial stage, chain mobility of pDCPD decreased slowly, which is typical of physical aging. The small amount of absorbed water caused no observable plasticization of pDCPD.

For epoxy composites (Fig. 3b), aging for two months caused the T_g to decrease significantly, from 101 °C to 84 °C, and the peak of the tan(δ) curve increased and broadened. These are marked features of plasticization - absorbed water molecules existed in a free state and acted as a lubricant, facilitating sliding between polymer chains. Continued aging for an additional ten months caused T_g to increase slightly, albeit to a much lower value than the pre-aged T_g. This slow increase in T_g can be partly attributed to post-curing and physical aging. Although the increase in peak height and width is not consistent with physical aging, the trend of T_g first decreasing and then increasing during aging has been reported in multiple studies of epoxy hygrothermal aging [22–26]. Some investigators have pointed out that this phenomenon can be caused by water molecules that strongly bond to polymer chains during long-term aging [22,23]. Fig. 3b also shows a small second peak at ~120 °C (arrow), which might result from this mechanism.

Matrix plasticization resulting from aging is also manifest by changes in fracture toughness. Plasticization decreases the matrix strength while simultaneously enhancing fracture toughness [10]. The enhanced fracture toughness can be beneficial to fatigue performance, because matrix cracking plays an important role in the damage accumulation process leading to fatigue failure [19]. Fig. 4 shows the evolution of K_{IC} for the neat polymer during aging. Note that the four groups of samples were aged and tested at the same time points - the data points are artificially offset to show symbols clearly. Similarly, an error bar is shown for only one data point (with the maximum error) for clarity. The K_{IC} of pDCPD decreased slightly (~10%) after aging for one year, and the embrittlement was attributed to thermal aging. The K_{IC} of epoxy, on the other hand, evolved in a markedly different fashion. The K_{IC} of the unaged epoxy was relatively low (about 30% of pDCPD), but increased significantly within the first three months, and was unchanged between the third and sixth months. After six months of aging, the evolution of K_{IC} was consistent with the evolution of water absorption (Fig. 2a) and T_g (Fig. 3b), indicating that the absorbed water caused matrix plasticization. However, after one year of aging, K_{IC} increased, despite the fact that saturation had been reached by six months of aging. The observed increase in K_{IC} occurred simultaneously with the appearance of the (second) small peak in the tan(δ) curve (Fig. 3b), and was tentatively attributed to strongly bonded water molecules. After one year of aging, the K_{IC} of the two resin systems was comparable.

3.2. Tensile strength degradation

Fig. 5 shows the static tensile strength evolution of 0° composites. In the graph, only the maximum error bar is shown for clarity.

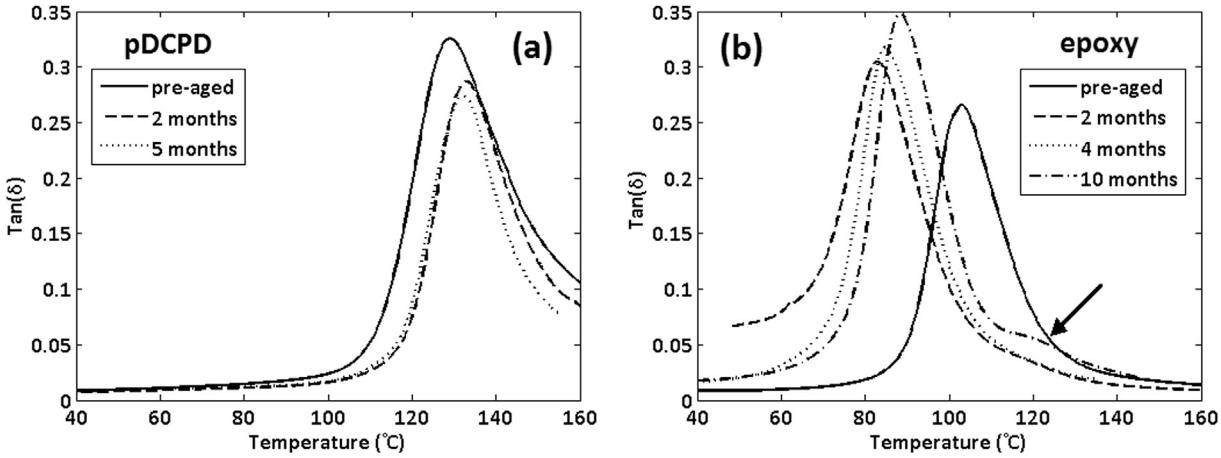

Fig. 3. Tan(δ) curve evolution during aging from DMA.

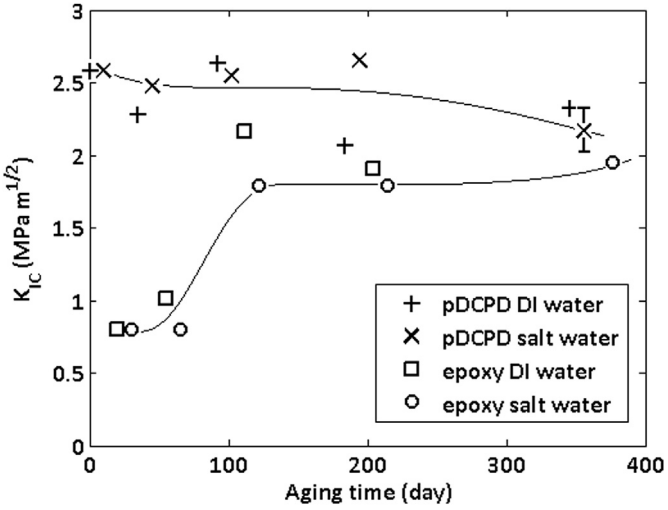

Fig. 4. Fracture toughness of neat cured resin.

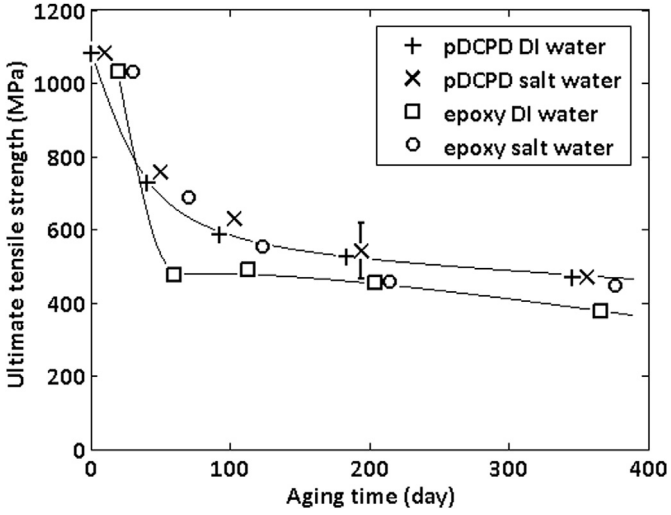

Fig. 5. Tensile strength evolution of 0° composite during aging.

The degradation of 0° tensile strength depends only on aging time, and is unaffected by the matrix type or aging environment. The only exception arises in the case of DI water aging of epoxy composites, where significant moisture absorption occurred. The average strength retention after one year of aging compared to the unaged condition is 42%, indicating significant loss of strength. The strength decrease is attributed to degradation of fiber strength, matrix strength and fiber-interface strength, because all three types of failure occur during 0° failure.

3.3. Fiber–matrix interface degradation

Fig. 6 shows the evolution of interface shear strength as a function of aging time, as determined from fiber push-out tests. Note that the aged samples were measured one year after they were removed from the aging environment, and although samples were stored in sealed plastic bags, some dehydration may have occurred. Thus, the interface strength values shown in Fig. 6 represent permanent interface damage, albeit in conditions different from the wet condition immediately after aging. (All other test data shown in this study were acquired at the end of each aging period.) The interface strength can undergo partial recovery during

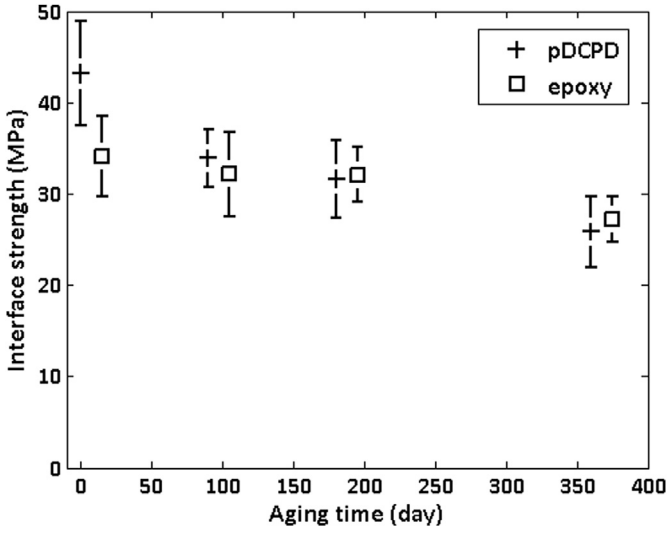

Fig. 6. Interface strength evolution from fiber push-out test (60 °C DI water).

this one-year storage period. The aging time points shown in Fig. 6 are 0, 3, 6 and 12 months - data points for the epoxy composite are artificially offset. Each data point represents 15 valid tests, and the error bars represent standard deviations.

Fig. 6 also shows that the interface shear strength (τ_{app}) of the glass/pDCPD composite prior to aging is similar to that of the glass/epoxy composite. The measured interface strength values prior to aging (43 MPa for pDCPD composites and 34 MPa for epoxy composites) are within the range of values previously reported from fiber push-out tests [32–34]. The value of τ_{app} decreases continuously with aging time for both composites, and continues decreasing after one year of aging, indicating the continuous damage to the interface caused by hygrothermal aging. The interface strength retention of pDCPD composites is 60% after one year of aging. The two composites show similar values of τ_{app} in the aged condition, although these values may differ from values measured immediately after aging.

Fig. 7 shows the short-beam strength (SBS) evolution with aging time. (Again, only the maximum error bar is shown for clarity.) The SBS depends both on the matrix shear strength and the interface shear strength, while the dependence on fiber strength is negligible because fiber breakage generally does not occur in interlaminar shear failure. Microscopic inspection revealed that failure occurred by delamination between plies due to shear, indicating valid test results. The pDCPD composite exhibited a slow and steady decrease in SBS with increasing aging time, and the integrity of the fiber interface was well-preserved. The retention of SBS for pDCPD composites after one year of aging is 85%, and this trend is consistent with the hydrophobicity of pDCPD matrix, as discussed previously. In contrast, epoxy composites showed a significant and continuous decrease in SBS during aging for one year, and the SBS after one year of aging decreased to 40% of the pre-aged value.

3.4. Combined aging effects on fatigue performance

The aging-induced degradation of matrix, fiber, and interface has been discussed in the preceding sections, and this section will focus on the combined effects on fatigue behavior. Fig. 8 shows a summary of *S–N* curves from 0° tension–tension fatigue tests. Fig. 8a shows data for pDCPD composites and Fig. 8b shows a comparison between pDCPD and epoxy composites. Data points with arrows indicate run-out samples. The two composites showed similar *S–N* curves for the pre-aged condition (solid lines), indicating comparable resistance to fatigue loading.

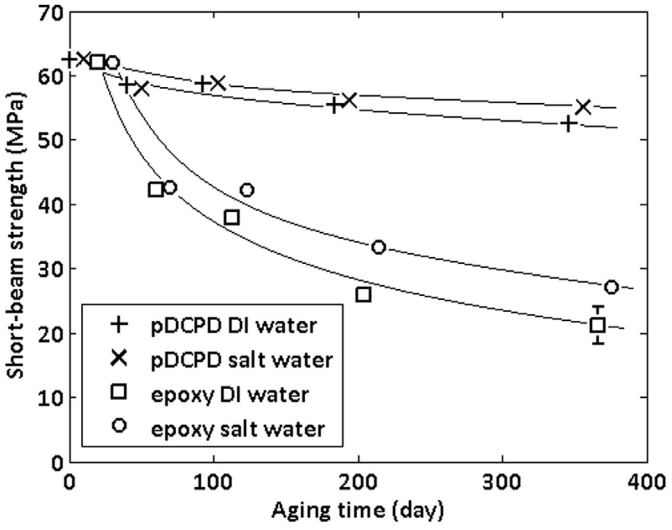

Fig. 7. Short-beam strength evolution during aging.

After one month of aging, the high-cycle fatigue (HCF) strength for pDCPD composites increased, while aging had a negligible effect on the low-cycle fatigue (LCF) strength. In general, damage accumulation at interfaces was the dominant factor controlling total high-cycle fatigue life. Thus, in the present case, the effect of matrix strengthening outweighed the effect of interface strength degradation and led to increased fatigue resistance of the composite. Additional factor worth mentioning is the possibility of water evaporation during fatigue test (>20 h). If the moisture content changes during fatigue testing, the fatigue behavior can differ from the "fresh wet" condition. However, because the sample temperature increases <3 °C during fatigue tests, the possible effect of any water evaporation is likely to be negligible. For LCF, water evaporation is negligible because of the short test times. In the LCF range, the number of loading cycles was relatively low, and the failure mode resembled static failure, in which fiber strength plays an important role. In this case, the effect of fiber strength decrease and matrix strengthening counterbalances, and thus the fatigue strength of the composite as a whole was unchanged.

After aging for one month, the HCF strength of epoxy composites remained unchanged, while the LCF strength decreased. The apparent stable HCF strength resulted from compensating effects of matrix toughening (Fig. 4) and interface degradation (Fig. 6). The LCF strength, on the other hand, decreased, because the effects of fiber and interface strength degradation outweighed the effect of matrix plasticization.

After 3 months of aging, the fatigue strength of both pDCPD and epoxy composites decreased significantly. The decrease can be attributed to three types of concurrent degradation: Matrix degradation, plasticization, oxidation and chain-scission cause the decrease in matrix strength. The glass fiber strength is also decreased, as evidenced by the strength drop in 0° composites. And the interface bonding is also weakened, as confirmed from single fiber push-out tests. The 0° fatigue strength degradation is interpreted as a combined effect of the degradation of all components in the composite. Both pDCPD and epoxy showed decrease in fatigue strength, although the pDCPD sample showed superior strength retention under similar aging conditions.

4. Conclusions

We have investigated the effects of hygrothermal aging on a ruthenium-catalyzed pDCPD neat polymer and glass fiber composite, using a traditional epoxy resin system as a benchmark material for comparison. The pDCPD matrix showed strengthening by thermal aging and resistance to water absorption. Consequently, pDCPD composites showed superior fatigue strength retention after long-term aging, especially in the high-cycle fatigue regime. In contrast, epoxy absorbed more water during aging and was significantly plasticized, resulting in significant decrease in the fatigue strength of the epoxy composite. For pDCPD composites, aging in salt water showed no different effects from aging in DI water, while salt water aging of epoxy composites showed less water absorption compared to aging in DI water.

The superior resistance of pDCPD composites to hygrothermal aging makes them suitable for potential applications in service environments involving exposure to moisture and high temperatures, including wind turbine blades, offshore oil platforms, protection shells for oil risers, and both marine and land vehicles. However, before such composites can be deployed in such applications, investigations are required to understand other types of aging and associated damage mechanisms, such as ultraviolet

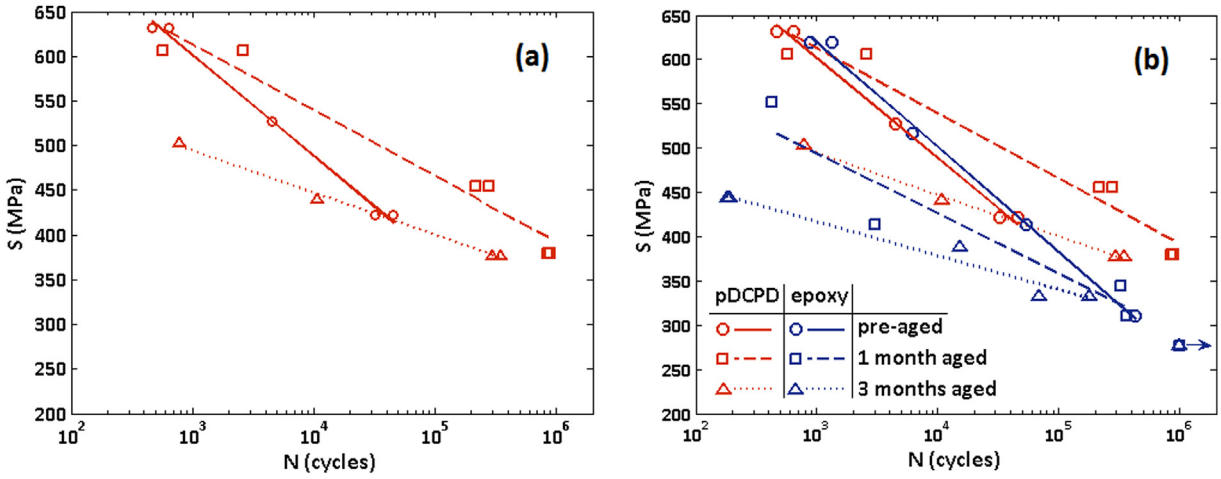

Fig. 8. Tension–tension fatigue *S–N* curve of 0° composite.

exposure, freeze-thaw cycling, thermal oxidation, and creep. For marine applications in particular, the possible effects of moisture on glass fibers and coatings must also be considered. Furthermore, in most practical applications, multiple types of aging occur concurrently and the effects couple, resulting in complex interactions and uncertain longevity. These interactions will have important implications for property retention and longevity in severe service environments. However, the intrinsic hydrophobicity of pDCPD coupled with the ease of infusion resulting from low resin viscosity offer distinct advantages over competing polymer in certain demanding applications, particularly those involving humidity, high temperatures, and cyclic loads.

Acknowledgments

Support from Materia Inc. (Pasadena, CA 91107, USA) is gratefully acknowledged. The authors thank Rohan Dhall and Dr. Matthew Mecklenburg from the Center for Electron Microscopy and Microanalysis (CEMMA) of University of Southern California for building the prototype of the fiber push-out tester. The authors also thank Patricio Martinez and Yuzheng Zhang from USC Composites Center for assistance in the fiber push-out tests.

References

[1] S. Kumar, K.V.V.S.M. Reddy, A. Kumar, G.R. Devi, Development and characterization of polymer-ceramic continuous fiber reinforced functionally graded composites for aerospace application, Aerosp. Sci. Technol. 26 (2013) 185–191.
[2] N.K. Kar, E. Barjasteh, Y. Hu, S.R. Nutt, Bending fatigue of hybrid composite rods, Compos. A 42 (2011) 328–336.
[3] N.K. Kar, Y. Hu, E. Barjasteh, S.R. Nutt, Tension-tension fatigue of hybrid composite rods, Compos. B 43 (2012) 2115–2124.
[4] R. Maurin, Y. Perrot, A. Bourmaud, P. Davies, C. Baley, Seawater ageing of low styrene emission resins for marine composites: mechanical behaviour and nano-indentation studies, Compos. A 40 (2009) 1024–1032.
[5] M. Deroine, A. Le Duigou, Y.M. Corre, P.Y. Le Gac, P. Davies, G. Cesar, S. Bruzaud, Accelerated ageing and lifetime prediction of poly(3-hydroxybutyrate-co-3-hydroxyvalerate) in distilled water, Polym. Test. 39 (2014) 70–78.
[6] P.Y. Le Gac, M. Arhant, P. Davies, A. Muhr, Fatigue behavior of natural rubber in marine environment: comparison between air and sea water, Mater. Des. 65 (2015) 462–467.
[7] E. Poodts, G. Minak, A. Zucchelli, Impact of sea-water on the quasi static and fatigue flexural properties of GFRP, Compos. Struct. 97 (2013) 222–230.
[8] E. Barjasteh, S.R. Nutt, Moisture absorption of unidirectional hybrid composites, Compos. A 43 (2012) 158–164.
[9] B. DeNeve, M.E.R. Shanahan, Water absorption by an epoxy resin and its effect on the mechanical properties and infra-red spectra, Polymer 34 (1993) 5099–5105.
[10] S. Alessi, D. Conduruta, G. Pitarresi, C. Dispenza, G. Spadaro, Accelerated ageing due to moisture absorption of thermally cured epoxy resin/polyethersulphone blends. Thermal, mechanical and morphological behaviour, Polym. Degrad. Stab. 96 (2011) 642–648.
[11] A.M. Figliolini, L.A. Carlsson, Mechanical properties of carbon fiber/vinylester composites exposed to marine environments, Polym. Compos. (2013).
[12] M.F. Arif, F. Meraghni, Y. Chemisky, N. Despringre, G. Robert, In situ damage mechanisms investigation of pa66/gf30 composite: effect of relative humidity, Compos. B 58 (2014) 487–495.
[13] M. Assarar, D. Scida, A.E. Mahi, C. Poilane, R. Ayad, Influence of water ageing on mechanical properties and damage events of two reinforced composite materials: flax–fibres and glass–fibres, Mater. Des. 32 (2011) 788–795.
[14] K. Liao, C.R. Schultheisz, D.L. Hunston, Long-term environmental fatigue of pultruded glass-fiber-reinforced composites under flexural loading, Int. J. Fatigue 21 (1999) 485–495.
[15] G. Kotsikos, J.T. Evans, A.G. Gibson, J.M. Hale, Environmentally enhanced fatigue damage in glass fibre reinforced composites characterised by acoustic emission, Compos. A 31 (2000) 969–977.
[16] P.Y. Le Gac, D. Choqueuse, M. Paris, G. Recher, C. Zimmer, D. Melot, Durability of polydicyclopentadiene under high temperature, high pressure and seawater (offshore oil production conditions), Polym. Degrad. Stab. 98 (2013) 809–817.
[17] A. Muhlebach, P.A. Schaaf, A. Hafner, F. Setiabudi, Thermal stability and degradation of hydrocarbon metathesis polymers, J. Mol. Catal. A Chem. 132 (1998) 181–188.
[18] B. Pan, J. Zhao, Y. Zhang, Y. Zhang, Dry sliding behaviors of polydicyclopentadiene under elevated sliding velocity, IERI Proc. 1 (2012) 19–24.
[19] Y. Hu, A.W. Lang, X. Li, S.R. Nutt, Hygrothermal aging effects on fatigue of glass fiber/polydicyclopentadiene composites, Polym. Degrad. Stab. (2014).
[20] F. McBagonluri, K. Garcia, M. Hayes, K.N.E. Verghese, J.J. Lesko, Characterization of fatigue and combined environment on durability performance of glass/vinyl ester composite for infrastructure applications, Int. J. Fatigue 22 (2000) 53–64.
[21] G.Z. Xiao, M.E.R. Shanahan, Swelling of DGEBA/DDA epoxy resin during hygrothermal ageing, Polymer 39 (1998) 3253–3260.
[22] J. Zhou, J.P. Lucas, Hygrothermal effects of epoxy resin. Part I: the nature of water in epoxy, Polymer 40 (1999) 5505–5512.
[23] J. Zhou, J.P. Lucas, Hygrothermal effects of epoxy resin. Part II: variations of glass transition temperature, Polymer 40 (1999) 5513–5522.
[24] M.A. Sawpan, P.G. Holdsworth, P. Renshaw, Glass transitions of hygrothermal aged pultruded glass fibre reinforced polymer rebar by dynamic mechanical thermal analysis, Mater. Des. 42 (2012) 272–278.
[25] T.S. Ellis, F.E. Karasz, Interaction of epoxy resins with water: the depression of glass transition temperature, Polymer 25 (1984) 664–669.
[26] V.M. Karbhari, G. Xian, Hygrothermal effects on high VF pultruded unidirectional carbon/epoxy composites: moisture uptake, Compos. B 40 (2009) 41–49.
[27] G.K. Schmitz, A.G. Metcalfe, Stress corrosion of E-glass fibers, Ind. Eng. Chem. Prod. Res. Dev. 5 (1966) 1–8.
[28] T.S. Chou, Stress-strain behaviour of physically ageing polymers, Polymer 34 (1993) 541–545.
[29] A.D. Drozdov, Physical aging in amorphous polymers far below the glass transition temperature, Comput. Mater. Sci. 15 (1999) 422–434.
[30] J.R. White, Polymer ageing: physics, chemistry or engineering? Time to reflect, C. R. Chim. 9 (2006) 1396–1408.

[31] M. Kharrat, A. Chateauminois, On the interfacial behaviour of a glass/epoxy composite during a micro-indentation test: assessment of interfacial shear strength using reduced indentation curves, Compos. A 28 (1997) 39–46.
[32] M.J. Pitkethly, J.B. Doble, Characterizing the fibre/matrix interface of carbon fibre-reinforced composites using a single fibre pull-out test, Composites 21 (1990) 389–395.
[33] X.F. Zhou, H.D. Wagner, S.R. Nutt, Interfacial properties of polymer composites measured by push-out and fragmentation test, Compos. A 32 (2001) 1543–1551.
[34] G.P. Tandon, N.J. Pagano, Micromechanical analysis of the fiber push-out and re-push test, Compos. Sci. Technol. 58 (1998) 1709–1725.